Thermodynamic study of MgSO4 – H2O system dehydration at low pressure in view of heat storage Author links open overlay

Larysa Okhrimenko, Loïc Favergeon, Kevyn Johannes, Frederic Kuznik, Michèle Pijolat

Thermodynamic study of $MgSO_4$ - H_2O system dehydration at low pressure in view of heat storage

Authors:

Larysa Okhrimenko[a], Loïc Favergeon[a], Kevyn Johannes[b], Frédéric Kuznik[c], Michèle Pijolat[a]

[a] Université Lyon, IMT Mines Saint-Etienne, Centre SPIN, CNRS, LGF, F - 42023 Saint-Etienne FRANCE

[b] Université de Lyon, Université Lyon 1, CETHIL UMR5008, F-69621 Villeurbanne, France

[c] Université de Lyon, INSA-Lyon, CETHIL UMR5008, F-69621 Villeurbanne, France

Corresponding author: E-mail address: favergeon@emse.fr

Abstract

Study about magnesium sulfate – water vapor equilibrium proved to be very interesting especially on the use of dehydration-hydration reactions for the heat storage application in recent research. Heat is realized by hydration of lower hydrates as this reaction is exothermic. Therefore, reversible reaction, endothermic thermal dehydration of higher hydrates, is used for charging of system and in this state the energy can be stored over long time. Even if magnesium sulfate appears as promising candidate with high theoretical energy density of 2.8 GJ/m^{-3}, technological process is rather complicated. The main problem that thermodynamic and kinetic data are poorly understood to present. In these study salt hydrates equilibrium of magnesium sulfate was investigated by new approach. It makes possible to understand the dehydration reaction of $MgSO_4 \cdot 6H_2O$ for heat storage application. Dehydration reaction under various water vapor pressures and temperatures were investigated by thermogravimetric analysis. The result showed that water content in the solid phase is a function of temperature for given water vapor pressure. So, we can conclude that this magnesium sulfate – water vapor system is bivariant and some hydrates appear as the non-stoichiometric hydrates.

Keywords: Thermodynamic model, $MgSO_4$, Thermogravimetry, Non-stoichiometry

Nomenclature:

m	sample mass (mg)
M	molar mass (g mol^{-1})
K	equilibrium constant
P	water vapor pressure (Pa)
ΔG	Gibbs free enthalpy of reaction (kJ mol^{-1})
ΔH	enthalpy of reaction (kJ mol^{-1})
T	temperature (K, °C)
R	gas constant (J K^{-1} mol^{-1})
F	number of degrees of freedom or variance
C	number of independent components
B	coefficient which depends on the temperature
H_2O_g	water molecules in the vapor phase
$H_2O_{H_2O}$	water molecule in normal position in the lattice
H_2O_i	water molecules in the interstitial position
V_{H_2O}	water vacancy
V_i	vacancy of interstitial position

Greek symbols

ε	total quantity of water remained in the solid per mole of low hydrate salt
φ	number of phases
χ	molar fraction
q	coefficient
γ	activity coefficient

1. Introduction

Could chemical reactions enable the energy transition from fossil resources to renewable energies? A sustainable energy transition means a shift to decentralized renewable energy and a more efficient energy use. Renewable energies allow reducing the consumption of fossil fuels and limiting the global warming increase. However, these sources are intermittent by nature. Energy storage systems are needed to shift the time between the supply and the energy demand. For example, the available solar energy exceeds the domestic demand during summer but during winter the total heating demand exceeds the solar supply. So, one role of energy storage systems could be to valorize the excess of solar energy in summer to fulfil the heat demand in the winter: it is interseasonal heat storage. Among the various technologies of heat storage, processes based on a reversible chemical reaction present the most important energy density [1] and are few impacted by heat losses during the storage time. Then, solid / gas reactions are good candidates for interseasonal heat storage.

A large number of potentially interesting materials has been performed in the last decade. Among all these reactive solid/gas systems, the couple magnesium sulfate/water vapor is presented as the most promising candidate [2-3]. The theoretical storage density of 2.8 GJ m^{-3} is realized by the dehydration/hydration of the following reaction:

$$\mathbf{MgSO_4\,(s) + 7H_2O\,(g) \leftrightarrow MgSO_4 \cdot 7H_2O\,(s)}.$$

However, the use of magnesium sulfate powder is difficult in a storage reactor because the particles rapidly form agglomerates during dehydration/hydration cycles, thus liming gas transfer and causing reversibility issues and low temperature lift. Therefore, system performance is consequently low [4]. To prevent an agglomeration of the powder as well as an augmentation of performance, a composite material was developed by impregnation of a hygroscopic salt (magnesium sulfate) into a porous matrix [5]. However, the development of such a system is technologically challenging. So before starting investigation of such materials, the data of hygroscopic salt/vapor system must be well known. Although extensive investigation of $MgSO_4/H_2O$ for heat storage application, the data about thermodynamics and kinetics of this system are, nowadays, incomplete in the literature.

The naturally occurring stable hydrated states in the $MgSO_4/H_2O$ system are epsomite ($MgSO_4 \cdot 7H_2O$), hexahydrite ($MgSO_4 \cdot 6H_2O$), kieserite ($MgSO_4 \cdot 1H_2O$) and products of total dehydration of high hydrates, $MgSO_4$ anhydrous. Other metastable hydrates ($MgSO_4 \cdot nH_2O$, where n=11, 5, 4, 3, 2, 5/4) can be produced synthetically under several conditions or by evaporation of aqueous solution of $MgSO_4$ [6–9]. Next investigation of synthetic $MgSO_4 \cdot 5H_2O$ is not possible because the compound decompose immediately in contact with the ambient atmosphere [10]. But for other new hydrates the thermodynamic data were calculated and experimentally determined by solution calorimetry.

Other authors showed that formation of $MgSO_4$ with 4, 2.4, 2, 1.25 and 1 H_2O molecules is possible by using the humidity buffer technique [11–14]. The experiments were performed using saturated salt solution which allows to control the relative humidity for different temperatures. Kinetic of these transformations is very slow and experiments duration were about weeks and months. $MgSO_4 \cdot 4H_2O$ was presented as a metastable hydrate that can also exist under special conditions. Formation of $MgSO_4 \cdot 1H_2O$ appears very difficult. Despite numerous attempts to obtain pure phase of $MgSO_4 \cdot 1H_2O$ by crystallization from a solution or by slow dehydration, mixture of various hydrates was formed instead [6, 15-16]. So, to prepare magnesium sulfate monohydrate, high hydrate like $MgSO_4$ hepta- or hexahydrate was dried at 350 °C and rehydrated under saturated salt solution.

The existence of other metastable hydrates was presented in the literature. $MgSO_4 \cdot 1.25H_2O$ or the five fourth hydrates or also called synthetic kieserite was synthetized by Emons [7]. Grindrod has analyzed a sample supplied as nominally 97% pure monohydrate of magnesium sulfate by Sigma-Aldrich but bulk composition significantly differed from $MgSO_4 \cdot 1H_2O$ [17]. Exact water content was determined by thermo-

gravimetric analysis. A sample was heated to 400 °C during 24 h to ensure total dehydration of material. Provided results show that water content corresponds to 1.36 moles of water per mole of $MgSO_4$. Then the XRD patterns was realized that allow to identify the presence of two hydrates: $MgSO_4 \cdot 1.25H_2O$ in large quantities and $MgSO_4 \cdot 2H_2O$ with a minor contribution; but it seems that $MgSO_4 \cdot 1H_2O$ is not present or is in very low quantity to be identify [11, 18]. In another case Wang listed the results obtained by gravimetric measurements of dehydration, with a water content of 1.18 and 1.09 mol H_2O per mol $MgSO_4$ for two different initial samples of so-called kieserite (called MH-1w and LH-1w) [12].

During dehydration reaction of $MgSO_4 \cdot 6H_2O$ to anhydrous magnesium sulfate in non-isothermal conditions and under dry or wet N_2 atmosphere, the hydrates with 0.1, 0.2 and 0.3 H_2O a priori were formed in the range of temperature between 250-275 °C [5, 18–20]. This phenomenon has not been well explained. In the same publications, in-situ XRD measurements are presented. The absence of lower hydrates of magnesium sulfate (i.e. less than 6 mol H_2O per mol $MgSO_4$) and the formation of an amorphous phase have been observed. The hypothesis proposed to explain this phenomenon is that the reorganization of the crystal structure is slow and inhomogeneous.

Donkers has studied the water transport on 1-2 mm crystal of heptahydrate of magnesium sulfate by NRM analysis in dynamic condition under dry N_2 atmosphere [22]. This analysis allows to show that liquid water is formed in the pore of crystal during dehydration at 48 °C due to local increase of the water vapor pressure. Aqueous solution formed inside the crystal influences the dehydration since deliquescence process occurs and the crystallization of new phase can be strongly affected. In the work conducted by van Essen [19], influence of various particle size distributions has been studied. It has been demonstrated that the particle size has a very important effect. Around the same temperature (~50 °C), an endothermic peak was observed with particle size distribution 200-500 µm that can be attributed to partial formation of liquid water inside the crystal. However, it seems that this process is typical only for large particles and is not found for small particles (<200 µm). In another study, the influence of low water vapor pressure on the kinetic rate of dehydration has been carried out [17]. It seems that the formation of the lower crystalline hydrates of magnesium sulfate is possible in special conditions like high relative humidity. The amorphous phase obtained by rapid dehydration of the high magnesium sulfate hydrates appears like metastable phase which can retain variable water content [21, 23]. It seems that lower hydrate obtained by rapid dehydration, follow its own dehydration process. It appears that dehydration process of $MgSO_4$ hydrates obeys to a bivariant system at low water vapor pressure while it occurs according to a monovariant one for high water vapor pressures. Although extensive investigation about $MgSO_4/H_2O$ system was realized for heat storage application, the data about thermodynamics and kinetics of this system are not well understood and incomplete in this research area. Indeed several metastable hydrated phases including content in water between 0 and 6 mol H_2O per mol $MgSO_4$ have been put in evidence. Nevertheless these crystalline phases have never been identified during thermal decomposition of solid magnesium sulfate hexahydrate in gaseous atmosphere and have been obtained by crystallization from aqueous solution or after deliquescence process.

In the present paper we report a new thermodynamic approach for better understanding the dehydration reaction for heat storage application. This approach is based on the non-stoichiometric model of hydrates [24]. Thermogravimetric analysis was used to study this system in isothermal-isobaric conditions.

2. Materials and methods

2.1. Sample and characterization

The material used throughout this study was magnesium sulfate hexahydrate beforehand in situ dehydrated from magnesium sulfate heptahydrate (VWR BDH Prolabo, CAS 10034-99-8, NORMAPUR, 99.5% pure). Three types of sample were used: the initial commercial powder grains (particle size is about 200-500 µm), crushed powder (particle size is about 5 µm) and pellet. Magnesium sulfate heptahydrate pellet was prepared by evaporation of aqua saturated solution of $MgSO_4 \cdot 7H_2O$. The solution was stored in small beaker of 28 mm diameter at ambient temperature. The crystal pellet was formed and then dried during two weeks in the laboratory ambiance. The specific surface areas were measured by means of the Brunauer-Emmet and Teller (BET) method from data obtained by nitrogen adsorption on a Micromeritics 2020 apparatus.

Powder XRD patterns of the samples ($5° \leq 2\theta \leq 50°$) were measured using a Bruker D8 Advance diffractometer with monochromatic Cu-Kα radiation (λ=1.54 Å) with a scan time of 5 s. The experimental

diffraction patterns were compared with known patterns of magnesium sulfate heptahydrate JCPDS 36-0419 and hexahydrate JCPDS 24-0719. Powder sample was placed on a platinum plate and exposed to dry air flow (50 mL min^{-1}). The sample was dehydrated by increasing the temperature from 25 °C to 60 °C using a heating rate of 1 °C min^{-1}. The XRD measurements were done at 25 °C and 30 °C then every 10 °C. Finally the sample was cooled to 24 °C and this temperature was remained constant during 24h.

2.2. Methods

Mass change data for the dehydration process were recorded using symmetrical suspension-type thermobalance from Setaram (MTB 10-8) in pure water vapor atmosphere. The water vapor pressure is maintained constant during each experiment using thermoregulated water bath. The water vapor pressure is imposed by the temperature, the total pressure being that of water vapor [25]. The thermobalance allows to estimate mass change with precision of about 0.001 mg. While the typical mass loss during an isothermal step is superior to 0.05 mg, the balance allows measuring the mass in temperature ramp properly. The sample-holder was a quartz crucible of 12 mm in diameter and a sample of crushed powder of about 2-3 mg (particle size ~5 µm) was introduced for each experiment. This initial sample mass was determined by preliminary measurements for different initial sample masses and allows to make experiments where the sample particles were dispersed over the bottom of the sample pan without forming any significant layer of sample particles. Thus, the undesired influences of mass and heat-transfer phenomena on the experimentally resolved shapes of mass-change curves and apparent kinetic behavior, which may possibly be caused by the diffusion of product gases through the sample bed and the thermal effects of the reaction, respectively, were expected to be negligible [26].

Two different temperature program patterns were applied to the measurement of the mass loss data: isothermal and stepwise isothermal conditions. Since magnesium sulfate heptahydrate is used as starting material, experiments were realized in two consecutive steps. Firstly, after introduction of the sample at room temperature, the vacuum (10^{-3} hPa) was carried out in the instrument for about 30 seconds. Then a pressure of water vapor equal to 21 hPa was established in the system in order to stabilize the sample mass. If the mass measurement is affected during pumping, the sample mass after establishment of the water vapor pressure of 21 hPa remains equal to the initial sample mass. After 15 minutes of stabilization at this pressure, the temperature was increased up to a given value (experimental range of temperature is 35-60 °C) and water vapor pressure was increased from 21 hPa to 25-100 hPa (depending on temperature to avoid water condensation). The temperature and water vapor pressure conditions were chosen so to be in the thermodynamic stability domain of magnesium sulfate hexahydrate (see Figure S1 – supplementary information).

In this condition, the first step of mass loss has been observed at about 7.2 ± 0.3 % and corresponds to the dehydration of magnesium sulfate heptahydrate into magnesium sulfate hexahydrate (theoretical mass loss is 7.3 %). Subsequently the water vapor pressure was decreased suddenly to the value chosen for the experiment by a short pumping and then maintained constant. The water vapor pressure stabilization takes about 15-30 seconds according to the chosen pressure. The mass loss for the dehydration of magnesium sulfate hexahydrate was thus registered in isothermal and isobaric conditions.

For stepwise isothermal method, after the same preliminary protocol, the mass loss occurring during dehydration is measured at a given temperature in isobaric conditions up to stabilization; the temperature is then increased and kept constant to a greater value and another mass loss is measured, etc. This procedure was repeated for several water vapor pressures.

After first step of mass loss, the resulting powder has been characterized by means of X-ray diffraction and the experimental diffraction pattern was successfully compared to known patterns of magnesium sulfate hexahydrate JCPDS 24-0719. To ensure that magnesium sulfate heptahydrate is completely reacted into hexahydrate but without partial dehydration to inferior hydrate, after first step of dehydration and mass stabilization, the sample has been heating to 350°C under dry N_2 atmosphere. When the sample was completely dehydrated to anhydrous magnesium sulfate, measured mass loss has been found to be 47.3± 0.3 % which correspond to 6 molecules of water (theoretical mass loss from hexahydrate to anhydrous magnesium sulfate is 47.32 %). Crystal phase has been characterized by X-ray diffraction and the XRD pattern matches the pattern of anhydrous magnesium sulfate (JCPDS 04-002-8228).

3. Results and discussion

3.1Sample characterization

Figure 1 shows in-situ X-ray diffraction patterns obtained during the dehydration of $MgSO_4 \cdot 7H_2O$ powder up to 60 °C. When the temperature is increased to 30 °C, appearance of $MgSO_4 \cdot 6H_2O$ phase was observed and then $MgSO_4 \cdot 7H_2O$ was completely transformed to $MgSO_4 \cdot 6H_2O$ at 40 °C. Above 50 °C an amorphous phase is formed, this observation is in good agreement with data from the literature [20]. Rehydration of amorphous phase was done at 24 °C and the end product after 24h corresponds to $MgSO_4 \cdot 6H_2O$.

Three samples with different particle sizes have been tested in order to study the influence of this parameter on the mass change occurring during dehydration process. The specific surface areas of the various samples measured by BET method are given in Table 1 and this data serve to explain the results presented in the Figure 4.

3.2 Reaction behavior

The curves representing mass loss versus time for the isothermal dehydration of magnesium sulfate hexahydrate commercial powder using various initial sample masses are presented in Figure 2. Mass-change curves obtained at 50 °C and 2 hPa exhibit a similar shape but kinetic behavior of samples with 5 and 11 mg are slower than samples with 2 and 3 mg. Therefore, samples with small initial mass present also satisfactory reproducible dehydration curve, so initial mass sample was chosen equal to about 3 mg for next experiments in this work.

Figures 3(a) and 3(b) represent the mass loss curves obtained in isothermal and isobaric conditions for different temperatures and different water vapor pressures respectively. The experiments performed at 40 °C, 50 °C and 60 °C and for a water vapor pressure of 2 hPa are presented in Figure 3(a), and the effect of water vapor pressure at 60 °C for 2, 5 and 10 hPa is shown in Figure 3(b). Experiments have been repeated at least 3 times. Estimated error doesn't exceed 1 % and as it has shown in Figure 2 the reproducibility is satisfactory.

The curves show a monotone decrease of the reaction rate during the dehydration progress for each experimental condition until the mass remains constant. As expected, the reaction rate increases with temperature and decreases with water vapor pressure. A surprisingly result is the difference of final mass loss for each experiment: 28.5% at 40 °C, 30.1% at 50 °C and 32.4% at 60 °C for 2 hPa of water vapor pressure; 32.7% at 2 hPa, 31.8% at 5 hPa and 30.5% at 10 hPa for 60°C. The end products were analyzed by XRD and for each dehydration experiment an amorphous phase was observed.

Figure 4 exhibits mass loss curves obtained for the dehydration of three samples (i.e. crushed powder, commercial powder and pellet) in the same temperature and water vapor pressure conditions. The experiments have been carried out at 40 °C for a water vapor pressure equal to 2 hPa. Even if the reaction rates are different, the final mass losses are the same for each sample despite their various specific surface areas (see Table 1).

So, Figures 3(a) and 3(b) allow to conclude that the final mass loss during dehydration of magnesium sulfate hexahydrate depends on both temperature and water vapor pressure and thus that the equilibrium between water vapor and the products of magnesium sulfate is bivariant. Figure 4 shows unambiguously that this bivariant equilibrium is not an adsorption phenomenon since the equilibrium state does not depend on the specific surface area of the sample (even with a factor more than 30). Coexisting phases are the solid solution of water molecules in magnesium sulfate and water vapor.

The dehydration reaction was then performed by means of isobaric and stepwise isothermal conditions. Figure 5 shows the mass loss versus time with changing the temperature at constant water vapor pressure of 5 hPa. The first step is performed at 45°C and the first mass loss observed is about 0.94 mg. Then the temperature was increased to 50°C which leads to a mass loss of 0.33 mg. The temperature values of 55, 60, 70 and 80 °C were achieved and for each step, the mass loss was measured. For each temperature step the mass remains constant after a sufficiently long time. These results confirm that water content in the solid phase is a function of temperature for a given water vapor pressure.

Thus, this system is bivariant and some magnesium sulfate hydrates appear as non-stoichiometric hydrates of $MgSO_4 \cdot 6H_2O$ solid phase. Equilibria can be represented by the following reaction:

$$\mathbf{MgSO_4 \cdot 6H_2O \leftrightarrow MgSO_4 \cdot \varepsilon\, H_2O + (6\text{-}\varepsilon)\, H_2O}$$

Using experimental data realized at various water vapor pressures and temperatures, the isobaric and isothermal curve of water content in the solid phase of magnesium sulfate can be determined from the mass change. Water content ε is defined as the total quantity of water remained in the solid per mole of low hydrate salt and is calculated by

$$\varepsilon = (\frac{m_{t,T,P}}{m_0} \cdot M_{MgSO_4 \cdot 6H_2O} - M_{MgSO_4})/M_{H_2O}$$

where $m_{t,T,P}$ represents the experimental mass loss at temperature T and water vapor pressure P, m_0 is the initial sample mass, $M_{MgSO_4 \cdot 6H_2O}$ is the molar mass of magnesium sulfate hexahydrate (228.46 g mol^{-1}), M_{MgSO_4} is the molar mass of anhydrous magnesium sulfate (120.37 g mol^{-1}) and $M_{H_2O}$is the molar mass of water (18 g mol^{-1}). Errors have been determined experimentally. The series of experiments have been repeated three times for all conditions. This has allowed us to determine the error-bar and the maximal value is about 3%. Results are presented by means of isobars (Figure 6a) and isotherms (Figure 6b).

All the results obtained by means of thermogravimetric analysis allow to plot the phase diagram of $MgSO_4$ - H_2O system by representing various isosteres (ε = constant) in a $P_{H_2O} - T$ diagram (Figure 7). Solid lines indicate a phase transition between crystalline phases [9, 25] and dash lines represent equilibrium curves for five chosen non-stoichiometric solids obtained in this work. The solid phase is considered as a solid solution of water molecules in the magnesium sulfate skeleton in equilibrium with the gaseous atmosphere.

3.3. Thermodynamic models of equilibrium between water vapor and hydrates

3.3.1 Gibbs' phase rule application

There are a lot of different inorganic salts able to fix water molecules. Equilibrium between two hydrates and water vapor can be presented as follow:

$$\boldsymbol{S \cdot (p+n)H_2O \rightleftarrows S \cdot nH_2O + pH_2O} \qquad \textbf{(I)}$$

where $\boldsymbol{p+n}$ and $\boldsymbol{n}$ are number of water molecules of two hydrate forms. The hydrate is anhydrous in the case $n = 0$.

The stoichiometric hydrates contain well-defined water content as integral part of the crystal lattice. Each hydrate has a well-defined crystal structure, different to their anhydrous solid or other hydrates. The non-stoichiometric hydrates have a variable composition in a given range without major corresponding change in their crystal structure.

For those systems in equilibrium, the Gibbs' phase rule is as follow:

$$\boldsymbol{F = C - \varphi + P}$$

where F is the number of degrees of freedom or variance (number of independent intensive variables), C is the number of independent components, P is the number of intensive variables and φ is the number of phases in thermodynamic equilibrium.

In both case the number of independent components is 2 (three components: two hydrates and water vapor, minus the number of reaction so 1). Number of intensive variables in the system is 2, i.e. temperature and water vapor pressure. In this system, there is one gaseous phase, so we can write $\boldsymbol{\varphi = \varphi_s + 1}$, where φ_s is the number of solid phase in equilibrium. So finally, Gibbs' phase rule can be given as:

$$\boldsymbol{F = C + P - \varphi_s - 1 = 3 - \varphi_s}$$

In the case of stoichiometric hydrates, there are two different solid phases in equilibrium represented by (I): two crystal structures, well defined, corresponding to each hydrate with $\boldsymbol{p + n}$ and $\boldsymbol{n}$ water molecules respectively. Consequently, $F = 1$, the system is monovariant and there is only one equilibrium water vapor pressure for a given temperature. However, for the non-stoichiometric hydrate case, there is one amorphous solid phase where hydrate forms with $\boldsymbol{p + n}$ and $\boldsymbol{n}$ water molecules are high and low limits. In this case, $F = 2$, the system is bivariant and there is a continuous change of solid phase composition with the water vapor pressure for a given temperature.

3.3.2 Stoichiometric hydrate equilibrium

In the general case, the decomposition of inorganic hydrate (and the corresponding hydration) is monovariant. The sorption isotherms are step-shaped and the pressure of the dehydration/hydration transition is a function of the temperature (Figure 8 (a)). In other words, if the temperature is fixed, there is only one equilibrium between two compositions for a given pressure.

Since the activities of both solid phases are equal to 1, the mass action law for equilibrium (I) can be written as:

$$\boldsymbol{K_I(T) = \frac{P_{eq}}{P^0} = e^{-\Delta G_I/RT} = K_I^0 e^{-\Delta H/RT}}$$

where P_{eq} is water vapor partial pressure at equilibrium in atm, P^0 is the reference pressure equal to 1 atm, $K_I(T)$ is equilibrium constant at temperature T, ΔG is the Gibbs free enthalpy of reaction, ΔH is the enthalpy of reaction. Associated enthalpy of transformation is generally positive so the dehydration is endothermic.

3.3.3 Non-stoichiometric hydrate equilibrium

Different authors have shown that, in particular conditions, the hydrate/vapor of inorganic and organic systems can be identified as bivariant [24, 27 – 31]. Typical isothermal curves representing the variation of the water content versus the water vapor pressure are reported in Figure 8 (b).

The thermodynamic properties of such a bivariant equilibrium between water vapor and solid hydrates have been studied by Soustelle [24, 33] by considering non-stoichiometry of the hydrates. The formulation of such thermodynamic models is based on the existence of solid solution [34, 35]. Two possible types of solid solution exist: substitution and interstitial. But these models seem to be the limit cases and have certain disadvantages as difficulty to identify the nature of all species. The model of non-stoichiometric hydrate allow total thermodynamic studying of solid/ water vapor equilibrium.The solid crystal is formed with quasi-chemical species and is described by structure elements using the Kröger-Vink notation [36].

Since hydrates are complex solid formed by at least three species (i.e. the anions, the cations and the water molecules), the choice was done to simplify it by considering a pseudo-binary system with the solid skeleton including water molecules not concerned by the equilibrium (n water molecules per salt molecule according to equation I) and the water molecules concerned by the equilibrium (p water molecules per salt molecule according to equation I).

Two models have been investigated to account for bivariant equilibrium between the water vapor and the solid hydrate via the non-stoichiometry approach. In the first case, all water molecules are assumed to be disordered and they can freely move from one position to another one. Thus water fills the space except the crystallographic positions of lower hydrate or anhydrous.

In the second model, the water molecules are localized on positions in the structure of the solid solution; two possibilities exist: under-stoichiometric hydrate with water vacancies and over-stoichiometric hydrate with water molecules on interstitial positions.

3.3.3.1 Non-stoichiometric hydrate with disordered and free water molecules

In this model, we assume that water molecules don't have a precise crystallographic position in the lattice. The water molecules are linked with the crystal lattice with relatively weak forces. For this reason they are easily mobile and can be removed or integrated into the structure without difficulty. Although the hydrate composition varies continuously, the change in the crystal structure is not significant. However, when loss of the water molecules in the solid becomes considerable, the non-stoichiometric hydrate loses its crystallinity.

We also consider that there is an interaction between water molecules. This interaction is quantified by a coefficient q, meaning that the water molecules can be associated in clusters of q molecules and one cluster of q molecules takes place on one site. The equilibrium is written as follow:

$$\boldsymbol{q\, H_2O_g \leftrightarrow (H_2O_i)_q} \qquad \textbf{(II)}$$

where H_2O_g is a water molecule in the gas phase and $(H_2O_i)_q$ is a non-localized and free water molecule in the solid phase.

According to the action law, the equilibrium constant is expressed as follow:

$$K_{II}(T) = \frac{P^q}{x_2 \gamma_2} \quad (1.1)$$

where $K_{II}(T)$ is the equilibrium constant at temperature T for equilibrium (II), x_2 is the molar fraction of water molecules, γ_2 their activity coefficient, and P is the water vapor pressure.
The molar fraction x_2 of free water molecules in the solid is the ratio between the quantity of free water molecules at time t and the total quantity of water molecules and is given by:

$$x_2 = \frac{\varepsilon - n}{q + \varepsilon - n}$$

where ε is an amount of water per mole of solid which may be changing during the transformation.

By substituting the x_2 value in equilibrium equation (1.1), the isotherm equation is written as:

$$\varepsilon = n + \frac{qP^q}{\gamma_2 K - P^q} \quad (1.2)$$

For ideal behavior of water molecules $\gamma_2 = 1$ and $q = 1$, the classical pathway of isotherm is presented in Figure 9 - curve 1. This isotherm presents a weak interaction between solid and water molecules. In the case $q > 1$ (see Figure 9 – curve 2) which correspond to condensate water in the solid, the isotherm shape is the same but the convexity is more important. Those properties are characteristic for crystal-soluble solids [37].

Equilibrium equation (1.1) with $\gamma_2 = 1$ is the easiest formulation but it doesn't give clear picture about interaction between water molecules and solid. Expression of regular solution using Margules' equation of second order [24] and third order [28] has been used for non-ideal solid solution. Even if third order Margules' equation gives a better fit in several cases, second order Margules' equation remains a good compromise ; the activity coefficients are given by:

$$ln\, \gamma_2 = B x_1^2 \quad (1.3)$$

where B coefficient depends on the temperature but is independent on the pressure and composition. It represents the interaction between the water molecules and solid of binary solution.

In equilibrium equation (1.2), by substituting the γ_2 expression, the isotherm equation becomes:

$$\varepsilon - n = \frac{qP^q}{Ke^{B[\frac{q}{q+\varepsilon-n}]} - P^q} \text{ or } \frac{P^q}{K} = \frac{\varepsilon - n}{\varepsilon - n + q} e^{B[\frac{q}{q+\varepsilon-n}]}$$

Curve 3 in Figure 9 is obtained in the case $B < 2$.The concavity of the shape change compared to curve 1 in Figure 9. It means that the water molecules are more attracted by the solid and therefore they loss their mobility in the solid. So, non-localized water molecules' model tends to localized water molecules' one.

3.3.3.2 Non-stoichiometric hydrate with localized water molecules

In this model of localized water molecules in the solid, there are two possible solutions. First, the water molecules occupy precise crystallographic position and some of these positions are not occupied. It means that the positions constitute vacancies of water molecules. Thus, the equilibrium between the solid phase and water vapor can be written as follow:

$$(H_2O_{H_2O})_q \leftrightarrow q\, H_2O_g + (V_{H_2O})_q \quad \textbf{(III)}$$

where $(H_2O_{H_2O})_q$ is a water molecule in normal position in the lattice, H_2O_g is the water vapor and $(V_{H_2O})_q$ is a water molecules vacancy.

In the second case, water molecules occupy interstitial positions in the lattice and equilibrium can be presented by:

$$q\, H_2O_g + (V_i)_q \leftrightarrow (H_2O_i)_q \quad \textbf{(IV)}$$

where $(V_i)_q$ is a vacancy of interstitial position, $(H_2O_i)_q$ is a water molecule occupying an interstitial position.

For example, the equilibrium constant for equation (III) is then given by:

$$K_{III}(T) = \frac{x_1 \gamma_1}{x_2 \gamma_2} P^q \tag{1.4}$$

$$x_1 = \frac{n+p-\varepsilon}{p+q}\,; \quad x_2 = \frac{\varepsilon - n}{p+q}$$

where $K_{III}(T)$ is the equilibrium constant at temperature T for equilibrium (III), x_1 and x_2 are the molar fractions of water vacancies and water molecules in the solid respectively, γ_1 and γ_2 their activity coefficients respectively, and P the water vapor pressure.

Soustelle [24] has shown that, in both case involving water molecule vacancies or interstitial water molecules, the expression of the isotherm is the same and can be written under the following form:

$$\varepsilon = n + \frac{p \frac{\gamma_1}{\gamma_2} P^q}{K + \frac{\gamma_1}{\gamma_2} P^q} \tag{1.5}$$

If the solid solution is assumed to be ideal ($\gamma_1 = \gamma_2 = 1$), there are two possible shapes of the isotherm $\varepsilon(p)$. In the first case $q \leqslant 1$, the curve monotonously increases (Figure 10 curve 4) and thus the concavity is inversed unlike the model with non-located water molecules. In the second case $q > 1$, the isotherm curve increases and has an inflection point (see Figure 10 curve 5).

If we introduce the variation of activities coefficient γ_1 and γ_2 as a function of composition $ln\gamma_2 = Bx_1^2$ for the activity coefficient of water molecules and $ln\gamma_1 = Bx_2^2$ for the activity coefficient of water molecules vacancies), it means that the interactions between water molecules and the solid skeleton increase. In the case $B < 2$ and $q \leqslant 1$, there is a very strong solid-water interaction. The isotherm is presented in Figure 11, curve 6, where the isotherm slope is very steep at low water vapor pressure and then reaches a plateau corresponding to saturation in the solid. In the other case $B > 2$ and $q \geqslant 1$, there is a repulsion between water molecules and the solid skeleton, and consequently separation between phases (lower and upper non-stoichiometric hydrates) is possible. This phenomenon is presented in Figure 11, curve 7, where both non-stoichiometric hydrates are separated by a monovariant transition.

The K, B and q values can be deduced from the experimental data of the water intercalation at different temperatures. Then the ΔH heat of water intercalation can be calculated from the obtained data.

3.4 Application of the model

As detailed in section 3.2, the values of $\varepsilon(P)$ were calculated from experimental mass change data and isotherms were plotted (Figure 6b). The shape of these isotherms is monotonously increasing. It corresponds to localized water molecules model of non-stoichiometric hydrate with $q \leq 1$.

By adopting the usual approximation of ideal solution behavior for the water molecules and vacancies, their activity coefficients γ_1 and γ_2, respectively, are equal to *1* whatever the temperature, pressure and composition. From the equation of the mass action law (Eq. 1.4), modifying accordingly with the assumption of ideal solution, and using that $p = 6$ (the maximum of sites for $MgSO_4 \cdot 6H_2O$) and $n = 0.1$ (the minimum sites observed without phase's transition [19]). The following power regression model between x_2 / x_1 and the pressure P can be deduced:

$$\frac{x_2}{x_1} = P^q \frac{1}{K} \tag{1.6}$$

The variations of x_2 / x_1 as a function of P at various temperatures are reported in Figure 12.

The q values as a function of temperature are presented in Figure 13. The value of q decreases linearly as the temperature increases. It means that the interaction between the molecules of water weaken with increasing the temperature. Departure of water molecules from normal position of crystal lattice is easier.

Knowing the q values at different temperatures and using the assumption of a strictly regular solid solution, the activity coefficients of binary mix obey the following relations:

$$\boldsymbol{ln\,\gamma_1 = Bx_2^2;} \qquad \boldsymbol{ln\,\gamma_2 = Bx_1^2} \tag{1.7}$$

where B is a coefficient depending on the temperature but which is independent of the pressure and composition.

According to this assumption and using previous values for p and n, the following equation can be rearranged into:

$$\boldsymbol{ln\frac{x_1}{x_2}P^q = lnK+(x_1^2 - x_2^2)B} \tag{1.8}$$

The plot of $ln\frac{x_1}{x_2}P^q$ versus $(x_1^2 - x_2^2)$ for each temperature are acceptably linear as shown in Figure 14. The slope value corresponds to coefficient B, that to say about intermolecular interaction, and y-intercept to $ln(K)$ which allows the determination of K, the equilibrium constant for each temperature.

The calculated values of q, B and K are given for each temperature in Table 2. The values of coefficient B are presented in Figure 13 as a function of temperature: B coefficient decreases with increasing the temperature. This observation is in agreement with the thermodynamic model, at very low temperature, when the value of B increase to 2, theoretically solid phase separation should occur. And in the other hand, at low value of B, the interaction between the last molecules of water and solid is in some measure stronger and dehydration needs the higher temperature.

The values of K are presented in Arrhenius coordinates in Figure 15. The values of $ln(K)$ increase linearly with increasing the temperature so the constant equilibrium K obeys to the Van't Hoff equation. The slope value correspondent to $-\frac{\Delta H^\circ}{RT}$ is -6.5313, so the enthalpy of the reaction is 54.3 kJ per mole of water. According to the literature data from Wagman [27] the enthalpy of dehydration of magnesium sulfate hexahydrate ($MgSO_4 \cdot 6H_2O$) to anhydrous magnesium sulfate ($MgSO_4$) is about 59 kJ per mole of water and the enthalpy of dehydration of magnesium sulfate hexahydrate to magnesium sulfate monohydrate ($MgSO_4 \cdot 1H_2O$) is about 55.1 kJ per mole of water. As the present work concerned hydrates with between 1 and 6 H_2O mol per $MgSO_4$ mol, the value of 54.3 kJ per mole of water is in good agreement with the literature data.

4. Conclusions

The present work reports the study of dehydration of magnesium sulfate at low water vapor pressure and the reaction mechanism that has been few studied in the literature. Dehydration of solid magnesium sulfate in a controlled atmosphere was monitored by thermogravimetry. The results obtained from these experiments show that the water content in the solid phase of magnesium sulfate varies with temperature at a constant water vapor pressure. At a constant temperature, the water content is a function of a water vapor pressure. This system is thus bivariant and some magnesium sulfate hydrates appear as non-stoichiometric hydrates. It explains the amorphous phase observation at low water vapor pressure in our work and in the previous studies [19]. Thermodynamic models were investigated for non-stoichiometric hydrates which explain an interaction between the water vapor and solid phase. Two general models of non-stoichiometric hydrates with disordered and localized water molecules have been presented with four possible equilibrium isotherms.

The results obtained for $MgSO_4$ hydrates are in good agreement with localized water molecules model with a q value lower than 1. The linear decrease of q with increasing temperature means that the interaction between the water molecules becomes weaker when the temperature increases. Moreover, B values decrease also with increasing temperature, thus the interaction between the water molecules and solid phase rises The equilibrium constant K was founded to follow Van't Hoff equation with the enthalpy of reaction ΔH = 54.3 kJ per mol of water. Application of this thermodynamic model allows to explain thermogravimetric dehydration curves of $MgSO_4 \cdot 6H_2O$ as well as the thermodynamic parameters.

5. Supplementary information.

The $MgSO_4/H_2O$ system

The phase diagram of $MgSO_4$ - H_2O system is presented in Figure S1, in consideration of the thermodynamic stable phases $MgSO_4 \cdot 7H_2O$, $MgSO_4 \cdot 6H_2O$, $MgSO_4 \cdot 1H_2O$ and anhydrous $MgSO_4$ [11, 26]. The solid black line corresponds to liquid/vapor water equilibrium; the dotted lines represent the equilibrium between stable solid phases; and dashed lines are the deliquescence humidity limits of $MgSO_4 \cdot 7H_2O$ and $MgSO_4 \cdot 6H_2O$ from [11]. Red and blue zones represent the experimental working conditions used in the present work: at first, formation of and secondly, the dehydration of $MgSO_4 \cdot 6H_2O$ respectively.

Equilibrium curves of $MgSO_4$ hydrates as a function of temperature and water vapor pressure can be approximated using the van't Hoff equation:

$$ln\frac{P_{H2O}}{P^0} = -\frac{\Delta_r H^\circ}{RT} + \frac{\Delta_r S^\circ}{R}$$

where $P^0$and P_{H2O} are the reference pressure (equal to 1 atm.) and the equilibrium pressure of water vapor respectively, ΔH_R^0 and ΔS_R^0 are the standard enthalpy variation and entropy variation respectively.

Recently metastable phase transition data like $MgSO_4 \cdot 6H_2O$ - $4H_2O$ has been added [11]. But formation of lower hydrates is possible only under special conditions. As it has been presented at the last studies of $MgSO_4$ - H_2O system for heat storage application, there is no observed formation of crystalline phase in this condition however amorphous phase which can be remain in this state. This is why these equilibrium curves are not presented in this paper.

Acknowledgements

The authors acknowledge "ARC Energy" from Region Rhône-Alpes for the funding.

7. References

[1] N. Yu, R. Z. Wang, and L. W. Wang, "Sorption thermal storage for solar energy," *Prog. Energy Combust. Sci.*, vol. 39, no. 5, pp. 489–514, 2013.

[2] K. E. N'Tsoukpoe, T. Schmidt, H. U. Rammelberg, B. A. Watts, and W. K. L. Ruck, "A systematic multi-step screening of numerous salt hydrates for low temperature thermochemical energy storage," *Appl. Energy*, vol. 124, pp. 1–16, 2014.

[3] T. Yan, R. Z. Wang, T. X. Li, L. W. Wang, and I. T. Fred, "A review of promising candidate reactions for chemical heat storage," *Renew. Sustain. Energy Rev.*, vol. 43, pp. 13–31, 2015.

[4] D. Gondre, K. Johannes, and F. Kuznik, "Inter-seasonal Heat Storage in Low Energy House: From Requirements to TESS Specifications," *Energy Procedia*, vol. 57, pp. 2399–2407, 2014.

[5] S. Hongois, F. Kuznik, P. Stevens, and J.-J. Roux, "Development and characterisation of a new $MgSO_4$–zeolite composite for long-term thermal energy storage," *Sol. Energy Mater. Sol. Cells*, vol. 95, no. 7, pp. 1831–1837, Jul. 2011.

[6] E. Balboni, R. M. Espinosa-Marzal, E. Doehne, and G. W. Scherer, "Can drying and re-wetting of magnesium sulfate salts lead to damage of stone?," *Environ. Earth Sci.*, vol. 63, no. 7–8, pp. 1463–1473, Aug. 2011.

[7] H.-H. Emons, G. Ziegenbalg, R. Naumann, and F. Paulik, "Thermal decomposition of the magnesium sulphate hydrates under quasi-isothermal and quasi-isobaric conditions," *J. Therm. Anal. Calorim.*, 2005.

[8] K.-D. Grevel and J. Majzlan, "Internally consistent thermodynamic data for magnesium sulfate hydrates," *Geochim. Cosmochim. Acta*, vol. 73, no. 22, pp. 6805–6815, 2009.

[9] K.-D. Grevel, J. Majzlan, A. Benisek, E. Dachs, M. Steiger, A. D. Fortes, and B. Marler, "Experimentally Determined Standard Thermodynamic Properties of Synthetic $MgSO_4 \cdot 4H_2O$ (Starkeyite) and $MgSO_4 \cdot 3H_2O$: A Revised Internally Consistent Thermodynamic Data Set for Magnesium Sulfate Hydrates," *Astrobiology*, vol. 12, no. 11, pp. 1042–1054, Nov. 2012.

[10] W. H. Baur and J. L. Rolin, "Salt hydrates. IX. The comparison of the crystal structure of magnesium sulfate pentahydrate with copper sulfate pentahydrate and magnesium chromate

pentahydrate," *Acta Crystallogr. Sect. B Struct. Crystallogr. Cryst. Chem.*, vol. 28, no. 5, pp. 1448–1455, May 1972.

[11] M. Steiger, K. Linnow, D. Ehrhardt, and M. Rohde, "Decomposition reactions of magnesium sulfate hydrates and phase equilibria in the $MgSO_4$–H_2O and Na^+–Mg^{2+}–Cl^-–SO_4^{2-}–H_2O systems with implications for Mars," *Geochim. Cosmochim. Acta*, vol. 75, no. 12, pp. 3600–3626, 2011.

[12] A. Wang, J. J. Freeman, and B. L. Jolliff, "Phase transition pathways of the hydrates of magnesium sulfate in the temperature range 50°C to 5°C: Implication for sulfates on Mars," *J. Geophys. Res.*, vol. 114, no. E4, p. E04010, Apr. 2009.

[13] S. J. Chipera and D. T. Vaniman, "Experimental stability of magnesium sulfate hydrates that may be present on Mars," *Geochim. Cosmochim. Acta*, vol. 71, no. 1, pp. 241–250, 2007.

[14] I.-M. Chou and R. R. Seal, "Magnesium and calcium sulfate stabilities and the water budget of Mars," *J. Geophys. Res.*, vol. 112, no. E11, p. E11004, Nov. 2007.

[15] M. Steiger, K. Linnow, H. Juling, G. Gülker, A. El Jarad, S. Brüggerhoff, and D. Kirchner, "Hydration of $MgSO_4 \cdot H_2O$ and Generation of Stress in Porous Materials," *Cryst. Growth Des.*, vol. 8, no. 1, pp. 336–343, Jan. 2008.

[16] K. Posern and C. Kaps, "Humidity controlled calorimetric investigation of the hydration of MgSO4 hydrates," *J. Therm. Anal. Calorim.*, vol. 92, no. 3, pp. 905–909, Jun. 2008.

[17] R. W. Ford and G. B. Frost, "The low pressure dehydration of magnesium sulphate heptahydrate and cobaltous chloride hexahydrate," *Can. J. Chem.*, pp. 591–599, 1956.

[18] P. M. Grindrod, M. J. Heap, A. D. Fortes, P. G. Meredith, I. G. Wood, F. Trippetta, and P. R. Sammonds, "Experimental investigation of the mechanical properties of synthetic magnesium sulfate hydrates: Implications for the strength of hydrated deposits on Mars," *J. Geophys. Res.*, vol. 115, no. E6, p. E06012, Jun. 2010.

[19] V. M. van Essen, H. A. Zondag, J. C. Gores, L. P. J. Bleijendaal, M. Bakker, R. Schuitema, W. G. J. van Helden, Z. He, and C. C. M. Rindt, "Characterization of $MgSO_4$ Hydrate for Thermochemical Seasonal Heat Storage," *J. Sol. Energy Eng.*, vol. 131, no. 4, p. 41014, 2009.

[20] H. Zondag, M. Van Essen, Z. He, R. Schuitema, and W. Van Helden, "Characterisation of $MgSO_4$ for thermochemical storage. Advantages of thermochemical storage."

[21] G. Whiting, D. Grondin, S. Bennici, and A. Auroux, "Heats of water sorption studies on zeolite–$MgSO_4$ composites as potential thermochemical heat storage materials," *Sol. Energy Mater. Sol. Cells*, vol. 112, pp. 112–119, May 2013.

[22] P. A. J. Donkers, S. Beckert, L. Pel, F. Stallmach, M. Steiger, and O. C. G. Adan, "Water Transport in $MgSO_4 \cdot 7H_2O$ During Dehydration in View of Thermal Storage," *J. Phys. Chem. C*, vol. 119, no. 52, pp. 28711–28720, Dec. 2015.

[23] S. J. C. David, T. Vaniman, "Transformations of Mg- and Ca-sulfate hydrates in Mars regolith," *Am. Mineral.*, vol. 91, pp. 1628–1642, 2006.

[24] M. Soustelle, *Thermodynamic modeling of solid phases*, vol. 3. ISTE Editions, 2015.

[25] L. Favergeon and M. Pijolat, "Influence of water vapor pressure on the induction period during $Li_2SO_4 \cdot H_2O$ single crystals dehydration," *Thermochim. Acta*, vol. 521, no. 1–2, pp. 155–160, Jul. 2011.

[26] S. Vyazovkin, K. Chrissafis, M. L. Di Lorenzo, N. Koga, M. Pijolat, B. Roduit, N. Sbirrazzuoli, and J. J. Suñol, "ICTAC Kinetics Committee recommendations for collecting experimental thermal analysis data for kinetic computations," *Thermochim. Acta*, vol. 590, pp. 1–23, Aug. 2014.

[27] D. D. Wagman, H. Evans, William, B. Parker, Vivian, H. Schumm, Richard, I. Halow, M. Bailey, Sylvia, L. Churney, Kenneth, and L. Nuttall, Ralph, "The NBS tables of chemical thermodynamic properties-Selected values for inorganic and C1 and C2 organic substances in SI units," *Phiysical Chem. Ref. Daa*, vol. 11, no. 2, p. 407, 1982.

[28] J.-R. Authelin, "Thermodynamics of non-stoichiometric pharmaceutical hydrates," *Int. J. Pharm.*, vol. 303, no. 1, pp. 37–53, 2005.

[29] J. J. Gardet, B. Guilhot, and M. Soustelle, "The dehydration kinetics of calcium sulphate dihydrate influence of the gaseous atmosphere and the temperature," *Cem. Concr. Res.*, vol. 6, no. 5, pp. 697–706, Sep. 1976.

[30] J. C. Mutin, G. Watelle, and Y. Dusausoy, “Study of a Lacunary Solid Phase l-Thermodynamic and Crystallographic Characteristics of its Formation,” *J. Solid State Chem.*, vol. 27, pp. 407–421, 1979.

[31] I. Nerád, I. Proks, and S. Šaušová, “Determination of equilibrium quantities of the systems formed by thermal decomposition according to the reaction A(cond),” *Chem. Pap.*, vol. 6, pp. 721–730, 1991.

[32] G. A. Stephenson, E. G. Groleau, R. L. Kleemann, W. Xu, and D. R. Rigsbee, “Formation of Isomorphic Desolvates: Creating a Molecular Vacuum,” *J. Pharm. Sci.*, vol. 87, no. 5, pp. 536–542, May 1998.

[33] M. Soustelle, J.-J. Gardet, and B. Guilhot, “La thermodynamique des hydrates cristallins : stoechiométrie. // The thermodynamic of solid hydrates: stoichiometry.,” *Séminaires Chim. l’Etat Solide*, vol. 6, pp. 32–50, 1972.

[34] C. A. Geiger, *Solid solutions in silicate and oxide systems of geological importance*. Eötvös University Press, 2001.

[35] C. Capobianco and A. Navrotsky, “Solid-solution thermodynamics in $CaCO_3$-$MnCO_3$,” *Am. Mineral.*, vol. 72, pp. 312–318, 1987.

[36] Kröger A. F., “The Chemistry of Imperfect Crystals. 2nd Revised Edition, Volume 1: Preparation, Purification, Crystal Growth And Phase Theory. North-Holland Publishing Company - Amsterdam/London 1973 American Elsevier Publishing Company, Inc. - New York 31,” *Cryst. Res. Technol.*, vol. 9, no. 7, pp. K67–K68, 1974.

[37] A. G. Tereshchenko, “Deliquescence: Hygroscopicity of Water-Soluble Crystalline Solids,” *J. Pharm. Sci.*, vol. 104, no. 11, pp. 3639–3652, 2015.

Tables

Samples	Specific area, $m^2.g^{-1}$
Crushed powder (~5 µm)	6.5
Grains (200-500 µm)	0.6
Pellet	0.2

Table 1.

T, °C	q	B	K
35	0.2723	0.892	0.1371
40	0.2668	0.740	0.1921
45	0.2570	0.513	0.2934
50	0.2482	0.480	0.3653
55	0.2441	0.410	0.5543
60	0.2386	0.287	0.6428

Table 2.

Figures

Figure 1. In-situ XRD patterns obtained at different temperatures during dehydration/hydration of magnesium sulfate.

Figure 2. TG dehydration curves for different initial sample mass performed at T=50°C and P(H_2O)=2 hPa.

Figure 3. TG dehydration curves: (a) at 2 hPa and different temperatures: 40 °C (green line), 50 °C (blue line) and 60 °C (red line) and (b) at 60°C for different water vapor pressure: 2 hPa (red line), 5 hPa (purple line) and 10 hPa (orange line).

Figure 3. TG dehydration curves: (a) at 2 hPa and different temperatures: 40 °C (green line), 50 °C (blue line) and 60 °C (red line) and (b) at 60°C for different water vapor pressure: 2 hPa (red line), 5 hPa (purple line) and 10 hPa (orange line).

Figure 4. TG dehydration curve at 2 hPa and 40 °C for different samples: crushed powder (purple line), grains (red line) and pellet (green line).

Figure 5. TG dehydration curve as a function of time at 5 hPa and stepwise isothermal heating.

Figure 6. a) Isobaric curve of the water content as a function of temperature for different water vapor pressure; b) Isothermal curve of the water content as a function of water vapor pressure for different temperature.

Figure 7. Phase diagram of the $MgSO_4$ - H_2O system. The solid lines enclose the areas of the stable phases according to the literature data; the dashed lines represent examples of isosteres obtained in the present work.

Figure 8. Dependences of the solid phase composition on temperature and gaseous pressure: a) monovariant equilibrium (three coexisting phases); b) bivariant equilibrium (two coexisting phases).

Figure 9. Isotherm of free water molecules model: (1) activity coefficient and q value is equal to 1, (2) activity coefficient is equal to 1, q value is greater than 1 and (3) activity coefficient follows Margules' second order equation.

Figure 10. Isotherm of located water molecules model with activity coefficient γ_1 and γ_2 is equal to 1: (4) q value $\leqslant$1, (5) q value >1.

Figure 11. Isotherm of located water molecules model with activity coefficient according Margules' second order equation: (6) B<2 and q $\leqslant$1; (7) B>2 and q $\geqslant$1.

Figure 12. x_2/x_1 as a function of water vapor pressure

Figure 13. q and B value as a function of temperature.

Figure 14. $ln\frac{x_2}{x_1}P^q$ as a function of $(x_1^2 - x_2^2)$

Figure 15. Variation of ln(K) as function of 1/T (K^{-1})

Figure S1. Phase diagram P_{H2O}(T) of $MgSO_4$ - H_2O

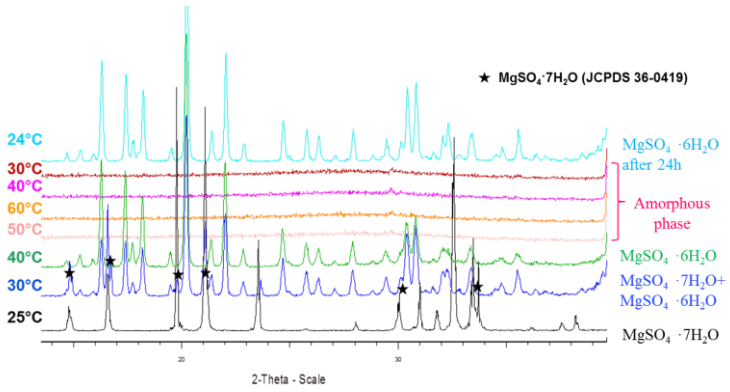

Figure 1.

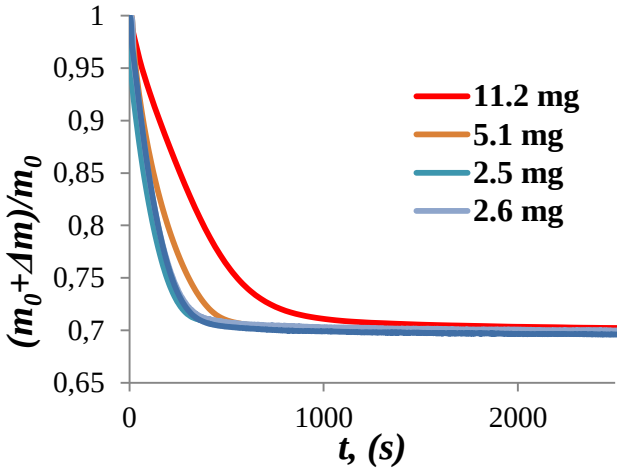

Figure 2.

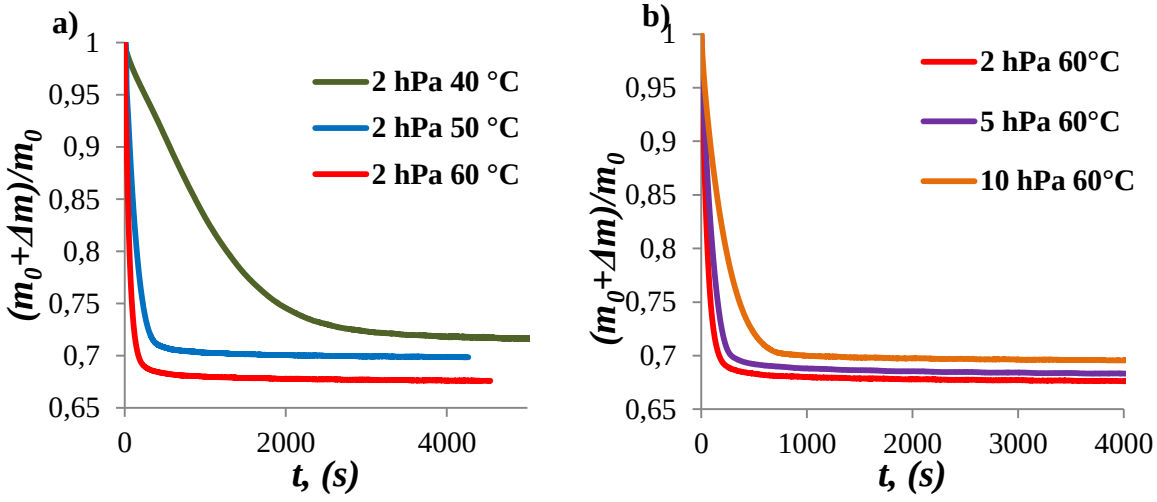

Figure 3.

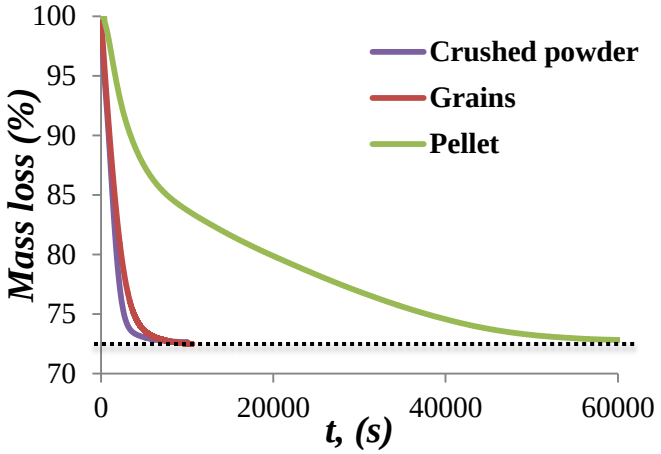

Figure 4.

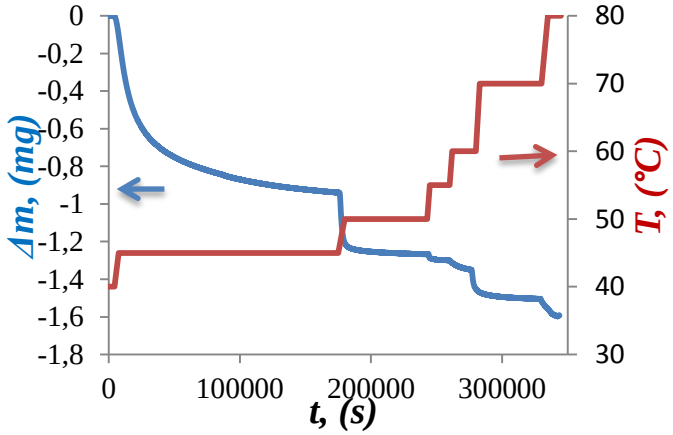

Figure 5.

a)

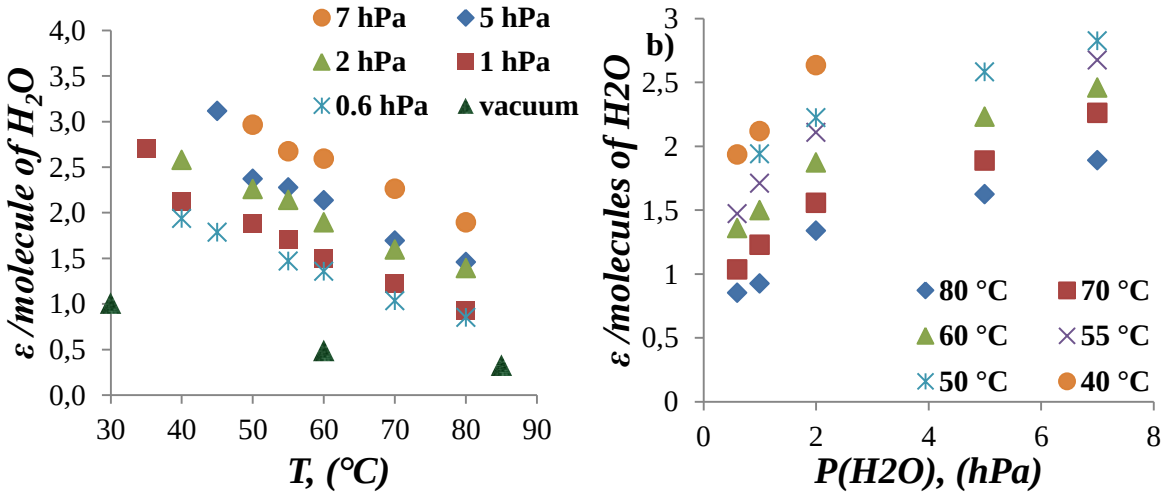

Figure 6.

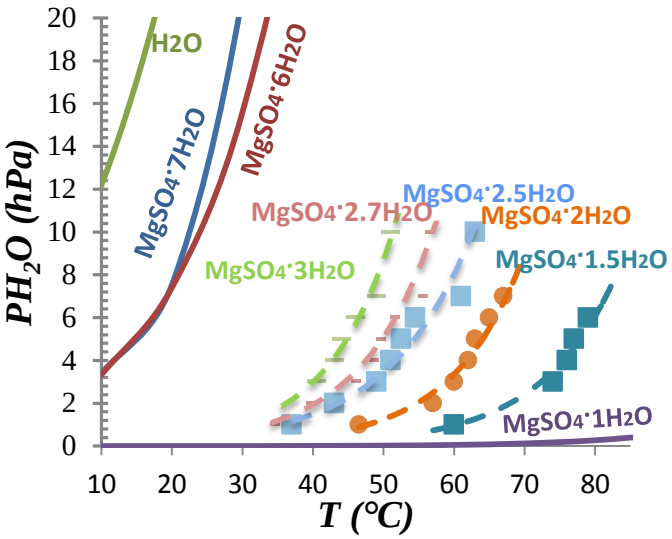

Figure 7.

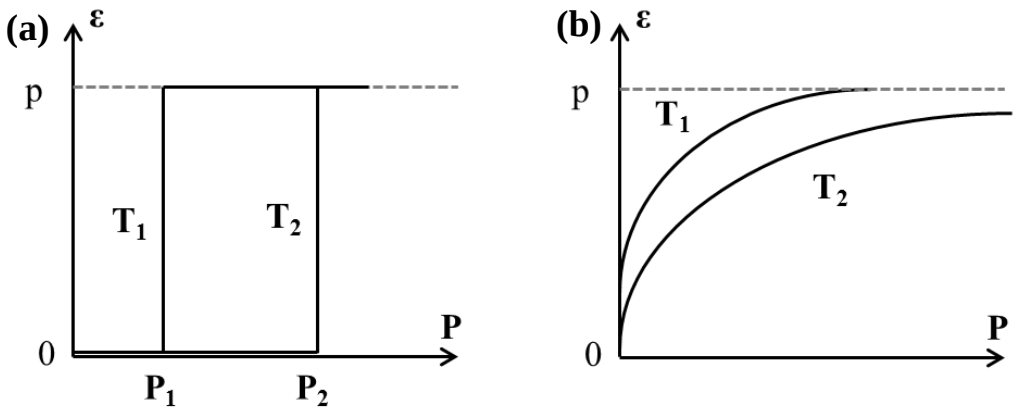

Figure 8.

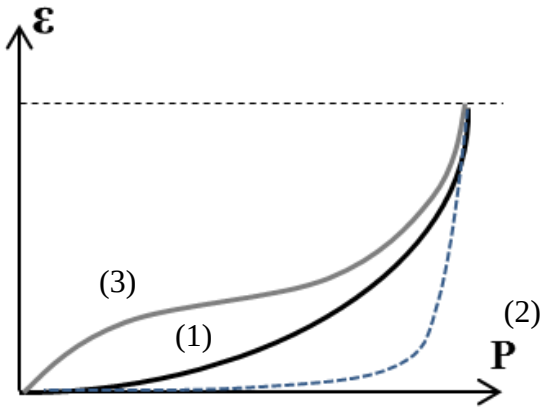

Figure 9.

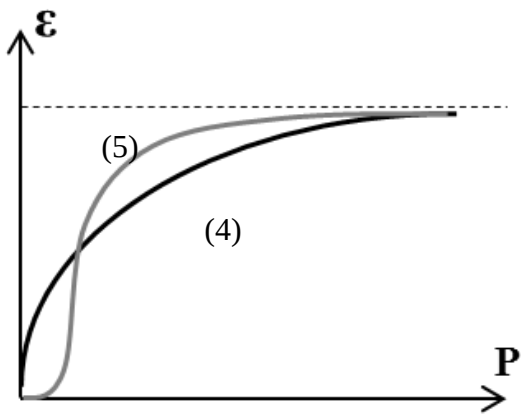

Figure 10.

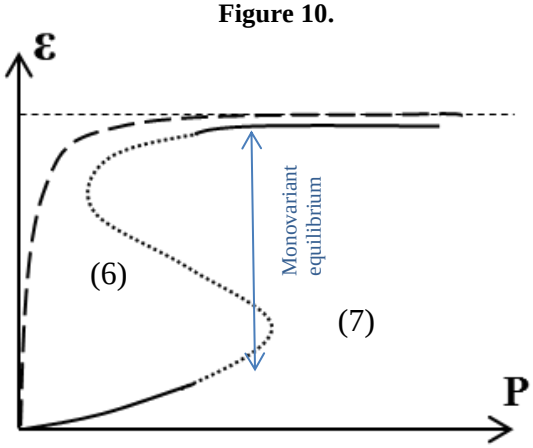

Figure 11

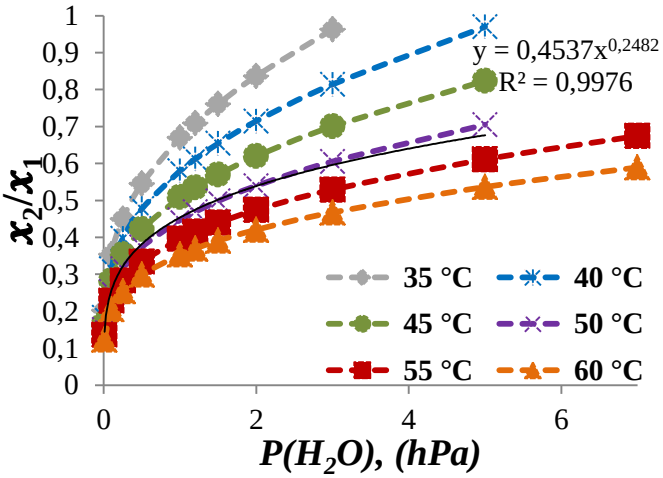

Figure 22.

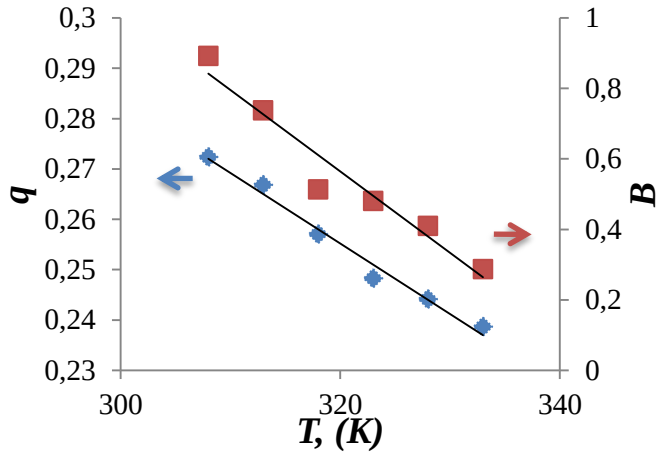

Figure 13.

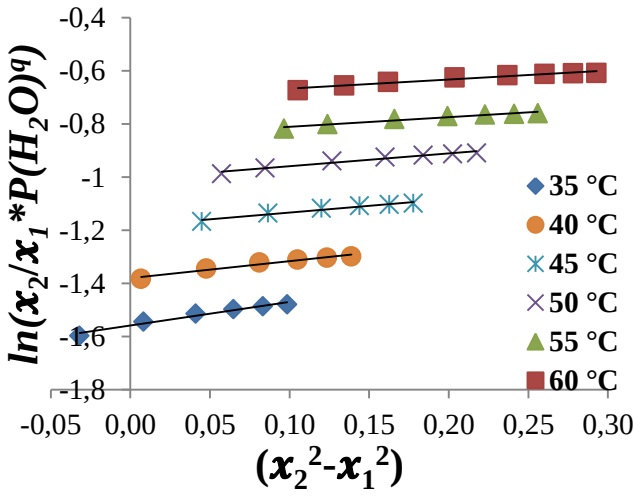

Figure 14.

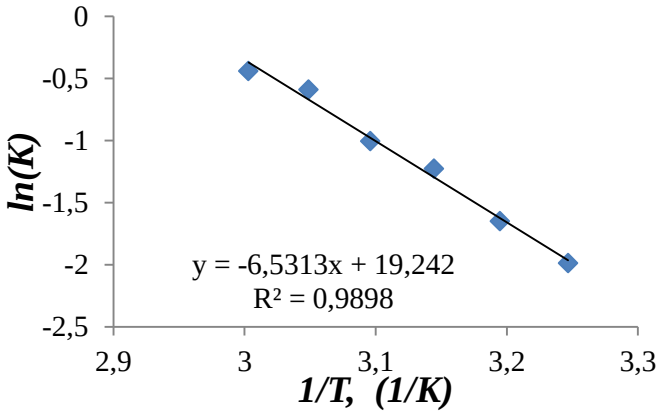

Figure 15.

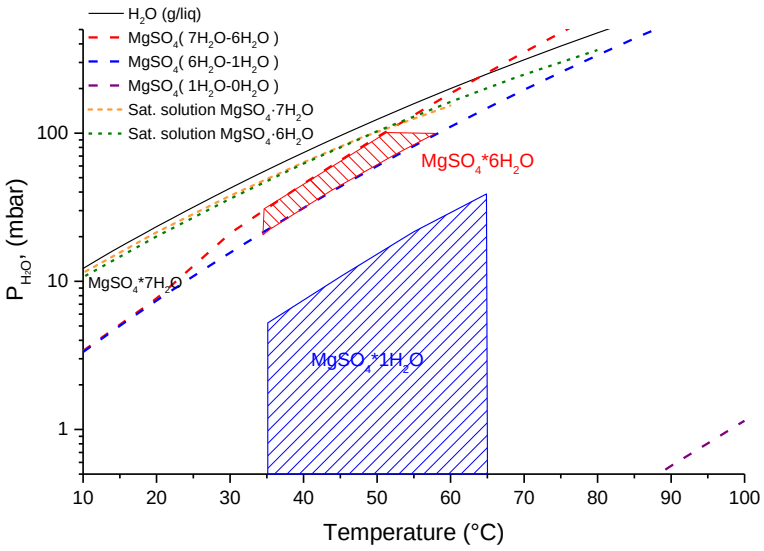

Figure S1.